Quantal-classical mixed-mode dynamics and chaotic behavior

Ersin Yurtsever
Chemistry Department, Middle East Technical University, Ankara, Turkey
(Received 6 May 1994)

Dynamical behavior of a nonlinearly coupled oscillator system is studied under classical and quantal-classical mixed-mode conditions. Classically, the system displays chaos above an energy threshold. However, upon a partial quantization of the problem within a self-consistent-field formalism, the dynamics becomes highly periodic, pointing out to the smoothing process of the quantum mechanics.

PACS number(s): 05.45.+b, 03.65.Sq, 82.20.Rp

INTRODUCTION

Intramolecular vibrational relaxation and energy redistribution (IVR) have been among the most challenging problems of chemical physics [1]. The description of the internal motion of molecules, such that the energy in certain mode(s) is transferred to other modes, forms the subject of molecular dynamics and the mechanisms and time scales of these processes pose interesting questions. These phenomena are almost invariably modeled by nonlinear equations and there are different approaches of establishing dynamical equations and their solutions. The most simple and widely used methodology is the classical trajectory analysis in which the Newton, Lagrange, or Hamilton equations are solved for the nuclear motion along the Born-Oppenheimer potential energy surface. Once the hypersurface is obtained from quantum mechanical methods of various sophistication, or by fitting to the experimental data, numerical integration techniques can then be employed to follow the motion of atoms in the $6N$-dimensional phase space [2]. Despite its general success, this approach has some serious drawbacks. First of all, as the system gets larger, the proper sampling of the phase space gets more and more difficult; that is, the necessary number of trajectories for a detailed analysis becomes too large for practical purposes. But more importantly, classical analysis suffers from its inability to incorporate several quantum effects such as zero-point vibration and tunneling. Exclusion of these effects may result in even qualitatively incorrect descriptions of the system for certain cases. For example, a classical system may dissociate by the transfer of energy from one mode to the dissociating mode, whereas in quantum description of the system, the amount of energy transferred would be less due to the zero-point effect, and one may not observe any dissociation at all. On the other hand, a full quantum calculation of the dynamics of a reasonably large molecule is computationally very prohibitive. Even though fast Fourier transforms allow us to carry out such a task, at least for small systems [3,4], the computational burden is too heavy to analyze anything but small molecules. There is a third alternative to molecular dynamics in which both highly developed techniques of the classical algorithms are employed and some quantum effects are included. In the so-called mixed-mode molecular dynamics, classical and quantum approaches are used together [5–9]. The basis of such a mixed-mode approach lies in the fact that in large systems there is a great variety of frequencies, which can roughly be classified as hard and soft modes, so that the hard modes are treated quantum mechanically whereas the slower ones can be studied within classical mechanical approaches. Once this separation is achieved, time evolution equations can be solved in a self-consistent-field methodology [10–12]. This is analogous to the Born-Oppenheimer approximation, in which the fast electronic motion is solved with quantum mechanical methodology for the fixed nuclei since they move relatively slower compared to electrons. Subscribing to this point of view, an N-dimensional problem can be written as a sum of smaller dimensional problems in which nonlinear terms appear as time-dependent perturbations.

There is also another very strong motivation of a detailed description of the mixed-mode dynamics. The classical behavior of the Hamiltonian systems is generally well understood with all the measures such as Poincaré maps, Kolmogorov or information entropy, and Lyapunov exponents allowing one to determine the regular and chaotic regimes in the phase space [13,14]. However, the quantum dynamics suffer from the lack of such well-defined measures, which distinguish the regular and "irregular" behavior [15–17]. The previously suggested measures, such as statistical analysis of the eigenvalue spectra [18,19], sensitivity analysis [20–22], or autocorrelation functions [23], do not strictly respond the way the classical mechanical counterparts work. In fact, the field of "quantum chaology" now no longer searches for the quantum chaos, but rather tries to distinguish different qualitative behavior in the dynamics [24–27]. Mixed-mode methodology offers an intermediate step in which one can study purely classical measures of a system under the effect of a quantum field. We would like to refer to this mixing as "partial quantization," rather than the more general "semiclassical approach." The idea is that after partitioning the modes, classical ones can be studied in two parallel sets of computations. The first one is the fully classical one (FC) and the other one is the mixed-mode (MM). In both methods, one set of modes remains classical but they move under the effect of "similar" classical and quantum fields. Therefore, it is now possible to

compare identical measures and observe changes upon partial quantization of the system.

MIXED-MODE DYNAMICS

Without loss of generality, let us begin with a two-dimensional oscillator system:

$$H(x,y)=H_x(x)+H_y(y)+V(x,y) , \tag{1}$$

where $V(x,y)$ is a nonlinear coupling term, and it is assumed that there is no transformation to obtain a separable form of the Hamiltonian. Within a self-consistent-field (SCF) approximation we obtain two one-dimensional Hamiltonians in the form of

$$H_x^{\mathrm{SCF}}=H_x+\langle V(x,y)\rangle_y , \tag{2a}$$

and

$$H_y^{\mathrm{SCF}}=H_y+\langle V(x,y)\rangle_x , \tag{2b}$$

where $\langle\ \rangle$ denotes an appropriate average over the remaining coordinate(s). Now the dynamical equations utilizing these operators can be solved iteratively, that is, the time evolution of the system along one coordinate is solved for a short time step under the influence of the average field of the other mode(s). Even though we do not have rigorous proof that the averaging process of SCF equations does not destroy chaotic behavior, our initial calculations show that classical trajectories of such a system do not show significantly different behavior than those of the original Hamiltonian if the time step is sufficiently small, even under chaotic conditions.

Once the new time-dependent SCF Hamiltonians are defined (since average quantities are constant only for the duration of the small time step, H_x^{SCF} and H_y^{SCF} are time dependent), it is now possible to combine quantum and classical dynamical equations with proper boundary conditions. If we choose the x coordinate to be the classical and y to be the quantum coordinate, our initial system is defined by a point in two-dimensional phase space (given by x and p_x) and a wave packet $\Psi(y,t)$ (for a better description of the classical motion, an ensemble of initial coordinates can also be employed). In that case, dynamical equations become

$$\partial p_x/\partial t=-\partial H_x^{\mathrm{SCF}}/\partial x , \tag{3a}$$

$$\partial x/\partial t=\partial H_x^{\mathrm{SCF}}/\partial p_x , \tag{3b}$$

and

$$i\hbar\partial\Psi(y,t)/\partial t=H_y^{\mathrm{SCF}}\Psi(y,t) . \tag{3c}$$

Choosing λx^2y^2 as the nonlinear coupling, we now define SCF Hamiltonians as

$$H_x^{\mathrm{SCF}}=H_x+\lambda\langle\Psi|y^2|\Psi\rangle x^2 \tag{4a}$$

and

$$H_y^{\mathrm{SCF}}=H_y+\lambda\{x^2\}y^2 . \tag{4b}$$

Here $\langle\ \rangle$ is the quantum average of y^2 over the wave packet and $\{\ \}$ is the square of the classical coordinate (again, for a bundle of trajectories, this is just an arithmetical average over all trajectories). The time evolution of classical trajectories can be obtained by the straighforward numerical integration techniques. The quantum equations can be solved by several methods. In order to carry out a systematic analysis, we decide to expand the initial wave packet as a linear combination of the eigenfunctions of the anharmonic oscillator H_y, and follow the time evolution again in terms of these basis functions. Our mixed mode system is chosen as [28,29]

$$\begin{aligned}H=&0.5(p_x^2+p_y^2+x^2+1.44y^2)-0.05x^3\\&+0.001\,406\,25x^4-0.0864y^3\\&+0.029\,16y^4+0.1x^2y^2 .\end{aligned} \tag{5}$$

The coefficients of the polynomial are chosen such that there are no double minima, and inflection points along each coordinate are at the same level. This Hamiltonian does not have any symmetry and there is no degeneracy in either one-dimensional or two-dimensional eigenvalue spectra. The wave packet is written as

$$\Psi(y,t)=\sum b_p(t)\varphi_p(y) , \tag{6}$$

where $\varphi_p(y)$ is the eigenfunction of H_y with quantum number p.

$$H_y\varphi_p(y)=\varepsilon_p\varphi_p(y) . \tag{7}$$

Now the Schrödinger equation in atomic units can be written as

$$i\sum\dot{b}_p\varphi_p(y)=\sum b_pH_y\varphi_p(y) , \tag{8}$$

with $\dot{b}_p$ denoting the time derivative of expansion coefficients. By multiplying with φ_q from the left and integrating over the coordinate, we obtain

$$i\dot{b}_q=\sum b_p A_{qp} , \tag{9}$$

where the matrix A is defined through

$$A_{qp}=\delta_{qp}\varepsilon_p+\lambda\{x^2\}\int\varphi_p(y)y^2\varphi_p(y)dy . \tag{10}$$

In matrix notation, we obtain

$$i\dot{B}=AB . \tag{11}$$

The above equation can then be simply solved by,

$$i\dot{B}=ACC^{-1}B . \tag{12}$$

Then,

$$iC^{-1}\dot{B}=C^{-1}ACC^{-1}B . \tag{13}$$

Defining $D=C^{-1}B$, we realize now a decoupled matrix equation,

$$i\dot{D}=ED , \tag{14}$$

where C is the pseudo-time-dependent unitary matrix that diagonalizes the Hermitian matrix A, E being a diagonal matrix with eigenvalues E_p. The solution is given as

$$d_p = N_p^0 \exp(-iE_p t) , \tag{15}$$

with N_p^0 being undetermined integration constants. Keeping in mind that the wave function must be continuous in time, that is,

$$\Psi^k(y,\delta t) = \Psi^{k+1}(y,0) , \tag{16}$$

k and $(k+1)$ define here two successive time steps. The boundary conditions can be expressed as

$$b_p^k(\delta t) = b_p^{k+1}(0) . \tag{17}$$

Then the final coefficients are

$$b_p^k(\delta t) = \sum C_{pm} d_m^{k+1}(0) , \tag{18}$$

and

$$d_m^{k+1}(0) = N_m^0 . \tag{19}$$

Finally, we obtain formulas for time-dependent coefficients of the wave packet

$$B^k = C^{k+1} N^{k+1} \text{ and } N^{k+1} = B^k (C^{k+1})^{-1} . \tag{20}$$

RESULTS AND DISCUSSION

In the Introduction, it is discussed that mixed-mode dynamics offers an extremely useful tool for the analysis of the irregular dynamics as we go along from the classical to the quantum world. By quantizing part of the Hamiltonian, one can still concentrate on the classical part of the system, that is, deterministic properties such as coordinates and momenta are analyzed instead of following the time evolution of average quantities of the quantum picture, which may give a completely different description due to the smoothing processes. Since definitions of classical measures like Poincaré maps or Lyapunov exponents of a mixed-mode system are somewhat ambiguous, we proceed to compute the usual quantities such as trajectories, time autocorrelation functions, and Fourier transforms of several observables of "similar" systems under fully classical (FC) and mixed-mode (MM) conditions. These conditions are defined as follows: for FC conditions, classical trajectories in the four-dimensional phase space are employed and for MM

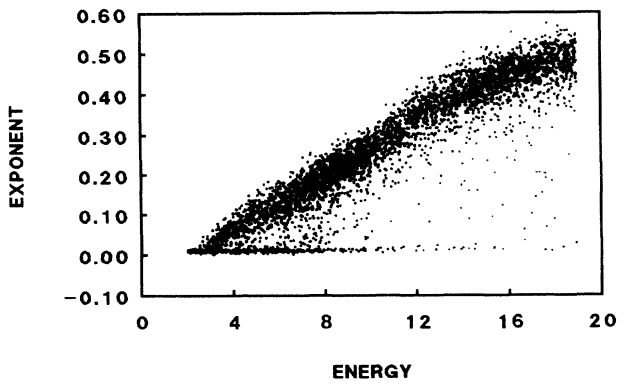

FIG. 1. Maximum Lyapunov exponents of the classical system.

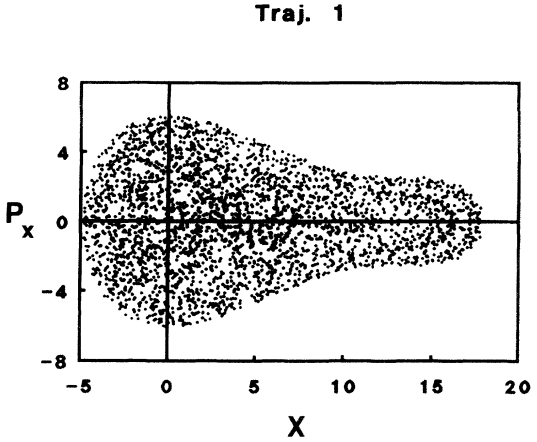

FIG. 2. Poincaré map of trajectory no. 1.

conditions, a combination of a classical trajectory in two-dimensions and a wave packet along the other coordinate forms the total system. In the model system, the x mode remains classical for both methodologies and the y mode is a quantal one for MM computations.

To summarize the classical behavior of this two-dimensional oscillator system, we present the Lyapunov exponent spectrum from 5500 trajectories as functions of the trajectory energy (Fig. 1). Lyapunov exponents are computed by the tangent space method [30,31], and the sum of all exponents remains less than 10^{-10} within our integration times of 500 units (10^5 steps). Throughout the discussion, generalized atomic units are employed and Lyapunov exponents are given in units of bits/time. Four-point constant-step Runge-Kutta integration is used to solve both nonlinear and linear equations. Lyapunov exponents generally converge around 250 units of time. At very low energies (there is only a single eigenvalue below 2.0 and 6 eigenvalues below 4.0), we start detecting positive Lyapunov exponents. The critical energy is around 8.0, after which there remains only a very small number of zero Lyapunov exponents. This small number of trajectories is attributed to initial conditions that are stuck in the deep valleys of the potential surface and can-

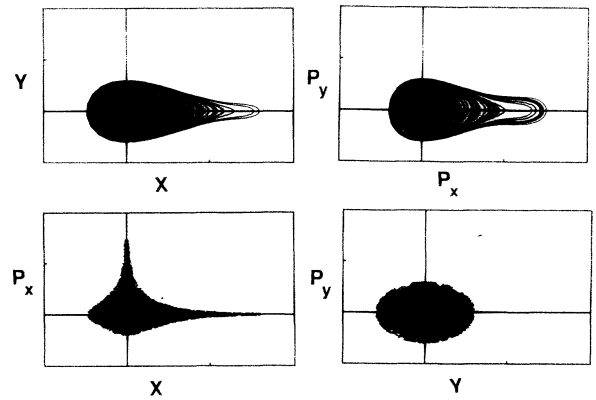

FIG. 3. Trajectory no. 1 along various cross sections of the phase space.

TABLE I. Initial conditions for classical trajectories.

Trajectory	y	P_y	E_y	E_c
1	1.943 652	1.655 468	3.497 499	0.023 611
2	−1.943 652	0.450 488	3.497 499	0.023 611
3	1.625 556	1.976 260	3.687 844	0.016 515
4	2.598 642	0.0	3.478 904	0.042 206

not escape within time scales of our numerical experiments. We conclude that the complete phase space is chaotic above this critical energy, and to fully realize the effects of quantization an energy value that lays in the completely chaotic regime is chosen for the comparison.

For the definition of the initial conditions for MM calculations, the coordinate and momentum along the x

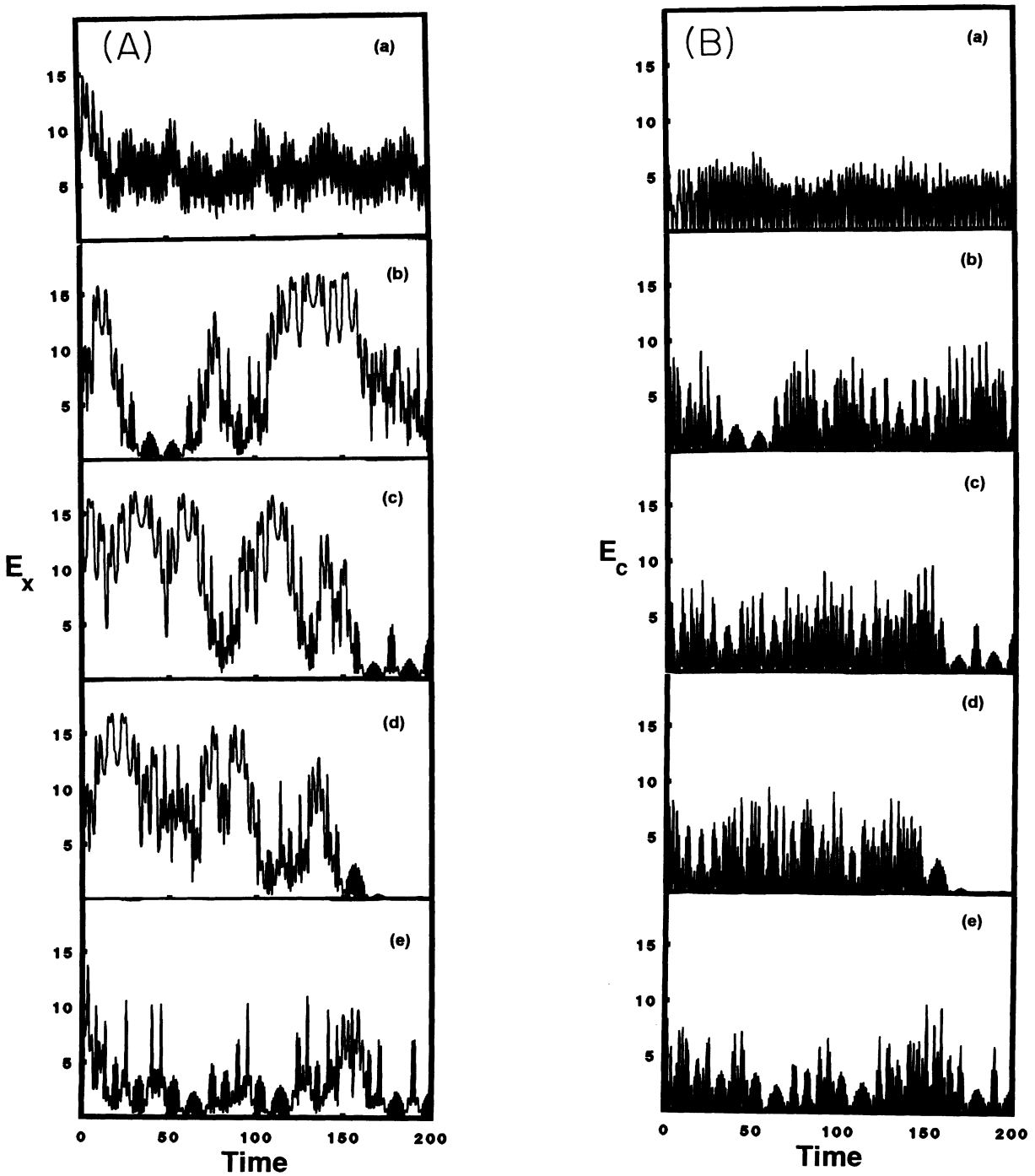

FIG. 4. (A) E_x for FC and MM trajectories. (a) Mixed mode, (b) trajectory no. 1, (c) trajectory no. 2, (d) trajectory no. 3, (e) trajectory no. 4. (B) E_c for FC and MM trajectories. (a) Mixed mode, (b) trajectory no. 1, (c) trajectory no. 2, (d) trajectory no. 3, (e) trajectory no. 4.

mode are chosen as $x=0.25$ and $p_x=5.471\,658\,94$, so that the classical energy is equal to 15.0. (Mode energies are computed only from Hamiltonians H_x or H_y, that is, the energy in the coupling is excluded.) Along the y mode, a wave packet as an equally weighed linear combination of the anharmonic oscillator eigenfunctions with quantum numbers 2 and 3 is used.

$$\Psi(y,0)=(1/\sqrt{2})(\varphi_2+\varphi_3)\ . \tag{21}$$

The quantum energy is then equal to 3.497 498 97, coupling energy is 0.023 611 15, and the total energy is 18.521 110 12.

The selection of the classical counterpart of the initial conditions for FC computations poses a severe problem;

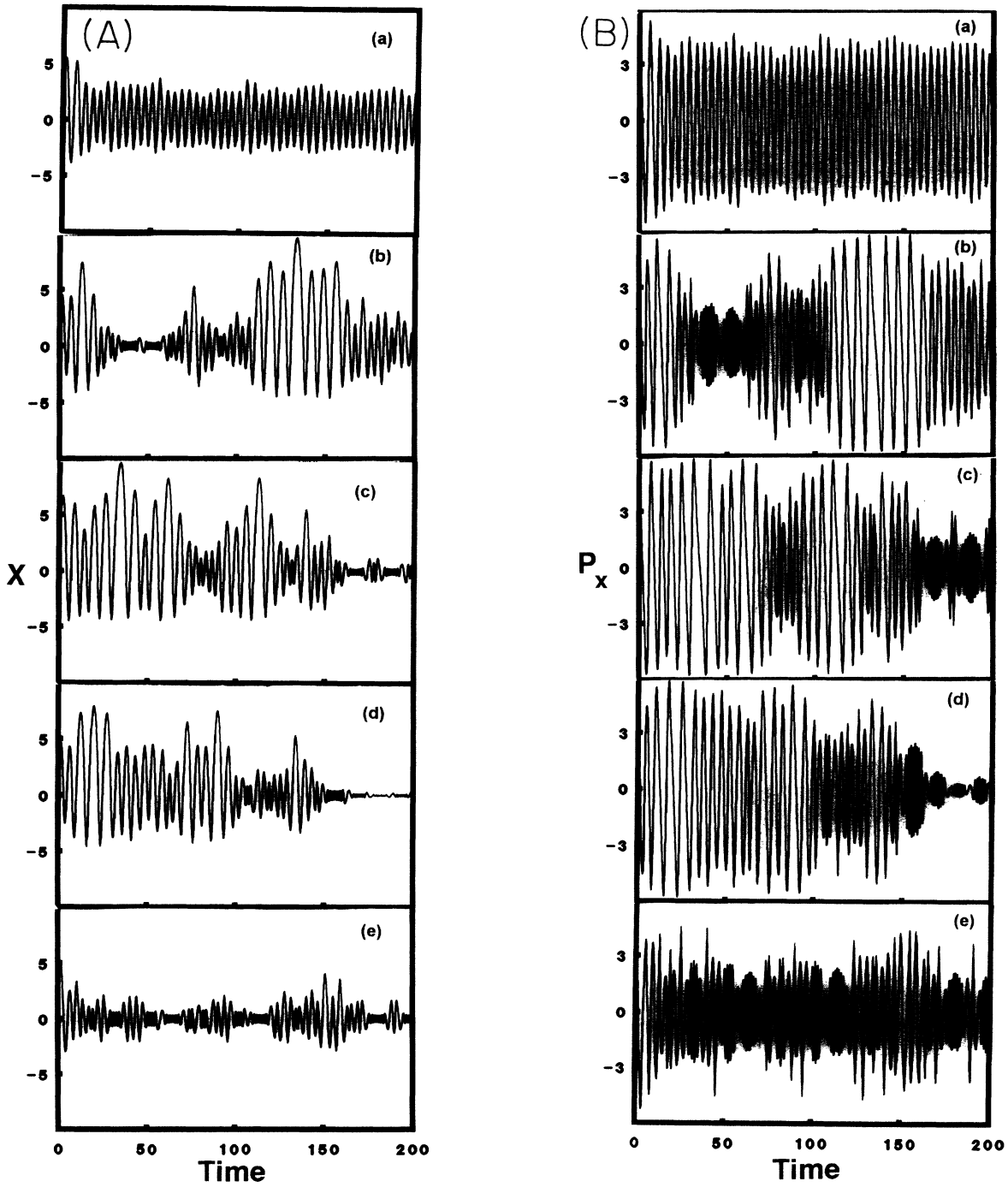

FIG. 5. (A) x for FC and MM trajectories. (a) Mixed mode, (b) trajectory no. 1, (c) trajectory no. 2, (d) trajectory no. 3, (e) trajectory no. 4. (B) p_x for FC and MM trajectories. (a) Mixed mode, (b) trajectory no. 1, (c) trajectory no. 2, (d) trajectory no. 3, (e) trajectory no. 4.

that is, we do not know an accepted way of choosing classical points that should correspond to a given wave packet. The Wigner transformations [32] in general can be used for such phase space representations; however, they suffer from the fact that they are not necessarily positive in all domains of the phase space, which makes them difficult to employ as probability distributions. In many cases, Husimi transformations [33–36] are proposed to sample the phase space, as they are positive definite in all regions, but they are of only intuitive nature. However, in this study, as we do not claim to exhaust the complete classical phase space, only a small number of trajectories are analyzed, and there may be different procedures of selecting these trajectories. We select four different FC trajectories whose energies are exactly the same as the MM case. These initial conditions are chosen such that

(a) and (b) the energy along the y coordinate and the coupling energy is the same in both the FC and MM cases; in this case, there are two y values with opposite signs (we choose only the positive momentum solutions).

(c) The classical y coordinate is the same as the expectation value over the wave packet.

(d) p_y is taken to be zero and y is obtained so that total energy is again the same.

Actual values of these coordinates and energy in modes and the coupling are given in Table I. These points sam-

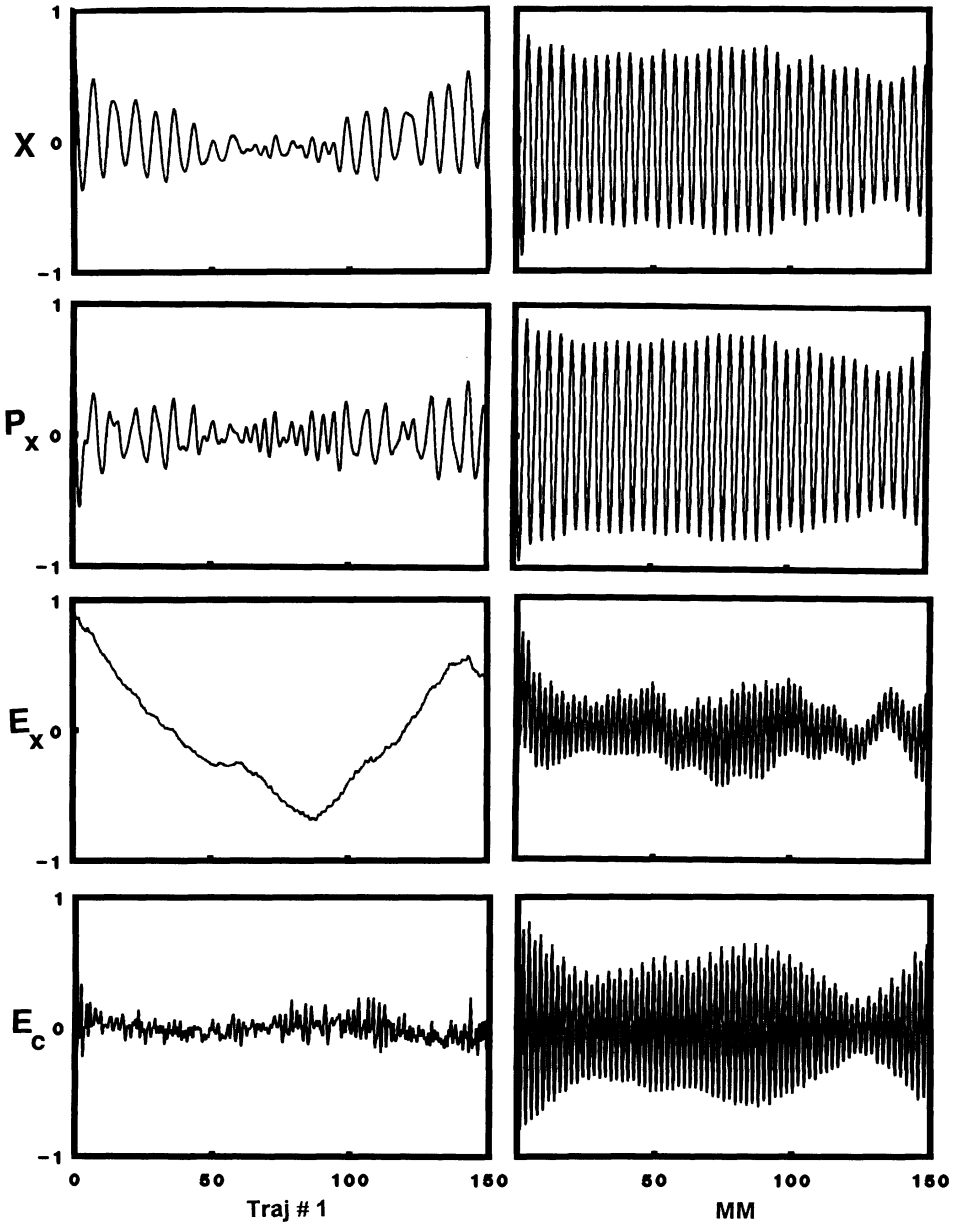

FIG. 6. Autocorrelation functions of x, P_x, E_x, and E_c for the classical trajectory no. 1 and MM.

ple the available phase space very sparsely, but as we see later they provide sufficient information on general trends. The maximum Lyapunov exponents for these initial conditions are 0.466, 0.449, 0.414, and 0.480 respectively. In Fig. 2, we present the Poincaré map, and in Fig. 3 various cross sections of the phase space for trajectory 1 are given. The other three trajectories give very similar trends, pointing out that indeed we are in the chaotic regime.

To compare two fundamentally different approaches poses some interesting problems, and one of them seems to be the partitioning of the coupling energy between two modes. That is, how does one define the energy of each mode? What are the contributions from the coupling energy? This separation is not unique and there is no standard method of determining the contributions to individual modes. Therefore, instead of computing energies of each mode in an arbitrary way, we proceed to define three energy terms E_x, E_y, and E_c, which are either classical observables, quantum expectation values, or a combination of them as in the case of E_c.

Since the x mode is always analyzed classically, it is more appropriate to compare properties of the FC and MM methodologies along the x coordinate. In Fig. 4, variations of E_x and E_c in time are given for the duration of 200 time units for the MM and four FC trajectories.

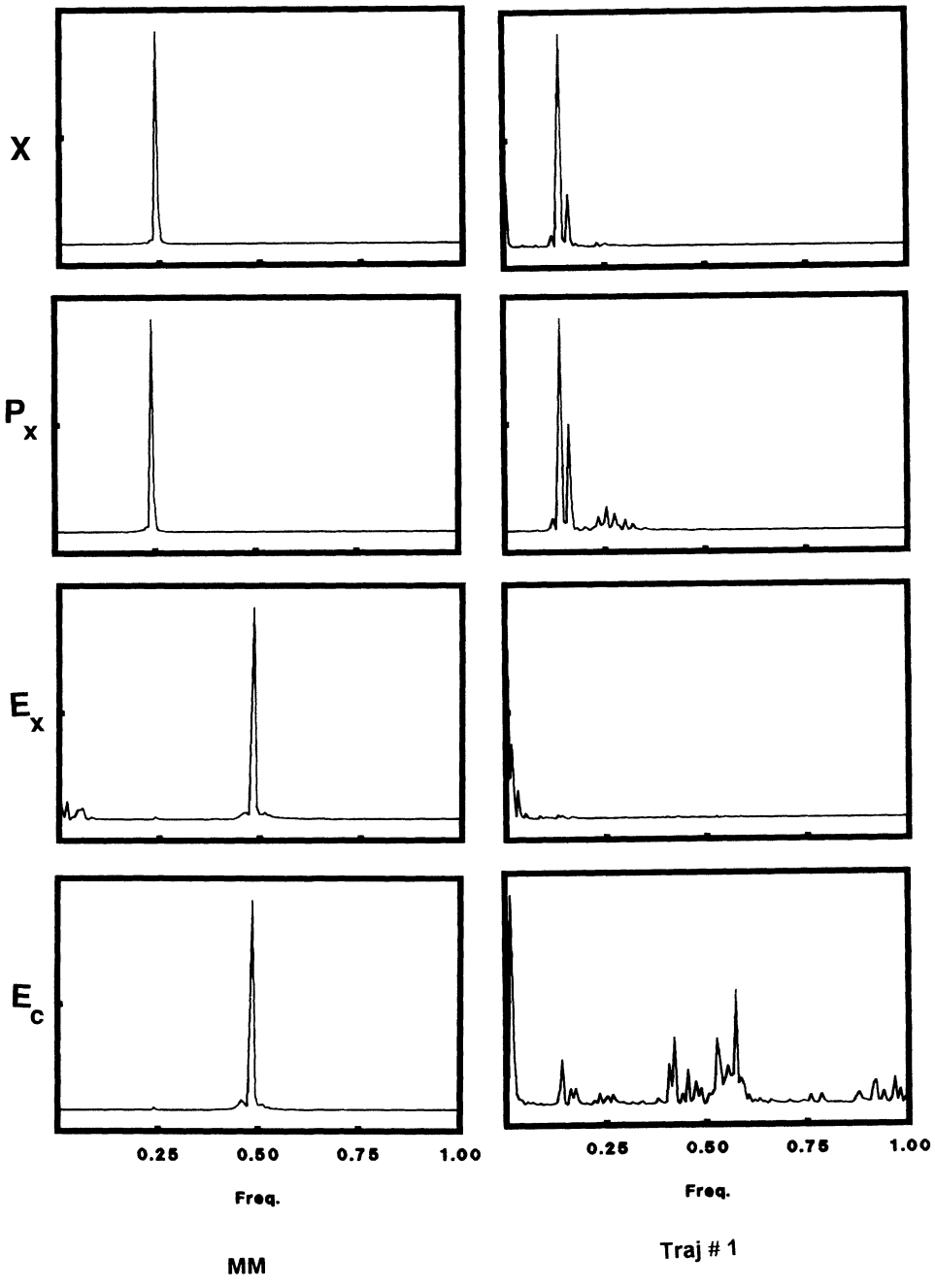

FIG. 7. Fourier transforms of autocorrelation functions of x, P_x, E_x, E_c.

We observe two types of distinct behavior. In all FC trajectories, both amplitudes and frequencies of the oscillations display a large variety (longer time series for these classical calculations are also carried out, but here only the relatively short ones are presented in order to be able to display details). However, in the MM methodology, it is clear that a great deal of periodicity appears in the corresponding time series. The variations of amplitudes are subdued and the very periodic looking structures are noted. In fact, they all seem to be composed of superpositions of a few similar frequencies. This qualitative change in the chaotic behavior is more pronounced for the coordinate and momentum along the x coordinate (Fig. 5) where the motion in the classical phase space seems to be only a single frequency one. In classical mechanics, chaos is recognized by the sensitivity of the initial conditions; that is, one asks the question of how fast the system forgets its past. One then can analyze the time autocorrelation functions, since they are thought to be memory functions.

$$C(\tau)=(1/N)\sum_{i=1}^{N} f(t)f(t+\tau)\ , \tag{22}$$

where f is the time-dependent function, τ is the correlation length, and N is the number of observations for the given τ. After normalization, $C(\tau)$ changes between -1 and 1, and any periodicity in it implies that the system still remembers its past history, which is a fingerprint of regular behavior. In Fig. 6, we display autocorrelation functions of x, p_x, E_x, and E_c for FC and MM cases. In classical calculations, autocorrelation functions go to zero quickly (sign of chaos) and then oscillate mildly around zero; however, those for the MM computations show strongly periodic structures. To determine the magnitudes of periodicity, we have obtained fast Fourier transformed (FFT) decompositions of autocorrelation functions (Fig. 7). As is expected, FFT transforms of FC trajectories show a variety of frequencies, whereas those of the MM trajectory display usually single sharp peaks. This final piece of evidence clearly points to a highly periodic and regular motion for MM dynamics.

We would like to summarize our findings in the following manner. In order to provide an opportunity to compare classical and quantum mechanical dynamics, we apply a mixed-mode formalism. Within this formalism, part of the system remains classical; therefore, exactly the same measures can be employed whether the system is fully classical or is under a partial quantization. For a reasonable comparison, we attempt to generate similar initial conditions for both approaches. Classical calculations under these conditions display highly chaotic behavior, as evidenced in the visual inspection of trajectories along a certain surface of sections and Lyapunov exponents. When we analyze several time-dependent properties, i.e., their autocorrelation functions and Fourier decompositions, we again note fingerprints of chaos. However, upon partial quantization, that is, by switching from the internal "classical" to "quantum" fields, radical changes in the qualitative behavior are observed. The time variations of classical energies and fields, radical changes in the qualitative behavior are observed. The time variations of classical energies and coordinates are no longer rich in frequencies, and they almost look "periodic." In fact, autocorrelation functions being highly periodic, we supply additional evidence to the disappearance of chaos, and FFT's fail to produce anything but single frequencies. It is reasonable to deduce from these facts that even a partial quantization smoothes out the chaotic details of a classical system. This is in accordance with our previous findings that a fully quantum description of a classically chaotic system displays a much more regular behavior than expected [28,29,37]. These results also provide additional evidence to the belief that bound systems of quantum systems cannot be chaotic [24,38].

ACKNOWLEDGMENTS

This project is supported by the TÜBiTAK, Grant No. TBAG-1218, as well as the NATO Grant No. GRG 900087. The author is grateful to J. Brickmann of Technische Hochschule Darmstadt for initiating this work.

[1] T. Uzer, Phys. Rep. **199**, 73 (1991).
[2] L. M. Raff and D. L. Thompson, *Theory of Chemical Reaction Dynamics,* edited by M. Baer (CRC, Boca Raton, FL, 1984), Vol. 3, p. 1.
[3] R. Kosloff, J. Phys. Chem. **92**, 2087 (1988).
[4] T. N. Truong, J. J. Tanner, P. Bala, J. A. McCammon, D. J. Kouri, B. Lesyng, and D. K. Hoffman, J. Chem. Phys. **96**, 2077 (1992).
[5] R. B. Gerber, V. Buch, and M. A. Ratner, J. Chem. Phys. **77**, 3022 (1982).
[6] R. Alimi, A. Garcia-Vela, and R. B. Gerber, J. Chem. Phys. **96**, 2034 (1992).
[7] A. J. Cruz and B. Jackson, J. Chem. Phys. **94**, 5715 (1991).
[8] E. Yurtsever and J. Brickmann, Ber. Bunsenges. Phys. Chem. **96**, 142 (1992).
[9] E. Yurtsever and T. Uzer, Ber. Bunsenges. Phys. Chem. **96**, 906 (1992).
[10] D. Farrelly and A. D. Smith, J. Phys. Chem. **90**, 1599 (1986).
[11] R. Alimi, R. B. Gerber, A. D. Hammerich, R. Kosloff, and M. A. Ratner, J. Chem. Phys. **93**, 6484 (1990).
[12] D. Farrelly and M. D. Emmel, Chem. Phys. Lett. **217**, 520 (1993).
[13] A. J. Lichtenberg and M. A. Lieberman, *Regular and Stochastic Motion* (Springer-Verlag, New York, 1993).
[14] M. C. Gutzwiller, *Chaos in Classical and Quantum Mechanics* (Springer-Verlag, Berlin, 1990).
[15] W. Dittrich and M. Reuter, *Classical and Quantum Dynamics* (Springer-Verlag, Berlin, 1992).
[16] F. Haake, *Quantum Signature of Chaos* (Springer-Verlag, Berlin, 1991).
[17] B. Eckhardt, Phys. Rep. **163**, 205 (1988).
[18] T. A. Brody, J. Flores, J. B. French, A. P. Mello, A. Pandey, and S. S. M. Wong, Rev. Mod. Phys. **53**, 385 (1982).
[19] T. Zimmermann, L. S. Cederbaum, H.-D. Meyer, and H. Köppel, J. Phys. Chem. **91**, 4447 (1987).

[20] N. Pomphrey, J. Phys. B **7**, 1909 (1974).
[21] D. W. Noid, M. L. Koszykowski, and R. A. Marcus, Ann. Rev. Phys. Chem. **32**, 267 (1981).
[22] J. Brickmann and R. L. Levine, Chem. Phys. Lett. **120**, 152 (1985).
[23] M. Shapiro, J. Ronkin, and P. Brumer, Ber. Bunsenges. Phys. Chem. **92**, 212 (1988).
[24] J. Ford and G.Mantica, Am. J. Phys. **60**, 1086 (1992).
[25] R. V. Jensen, Nature **355**, 311 (1992).
[26] W. H. Zurek, Phys. Today, **44** (10), 36 (1991).
[27] W. Slomczynski and K. Zyczkowski (unpublished).
[28] E. Yurtsever and J. Brickmann, Phys. Rev. A **41**, 6688 (1990).
[29] E. Yurtsever and J. Brickmann, Ber. Bunsenges. Phys. Chem. **94**, 804 (1990).
[30] J. Tobochnik and H. Gould, Comp. Phys. **3** (6), 86 (1989).
[31] A. Wolf, J. B. Swift, H. L. Swinney, and J. A. Vastano, Physica D **16**, 285 (1985).
[32] E. Wigner, Phys. Rev. **40**, 749 (1932).
[33] K. Husimi, Proc. Phys. Math. Soc. Jpn. **22**, 264 (1940).
[34] K. Zyczkowski, Phys. Rev. A **35**, 3546 (1987).
[35] K. Takahashi and N. Saito, Phys. Rev. Lett. **55**, 645 (1985).
[36] P. Al Jalil and E. Yurtsever, Tr. J. Phys. (to be published).
[37] E. Yurtsever, *Integrability and Chaotic Behavior,* edited by J. Seimenis (Kluwer, Dordrecht, in press).
[38] J. Manz, J. Chem. Phys. **91**, 2190 (1989).

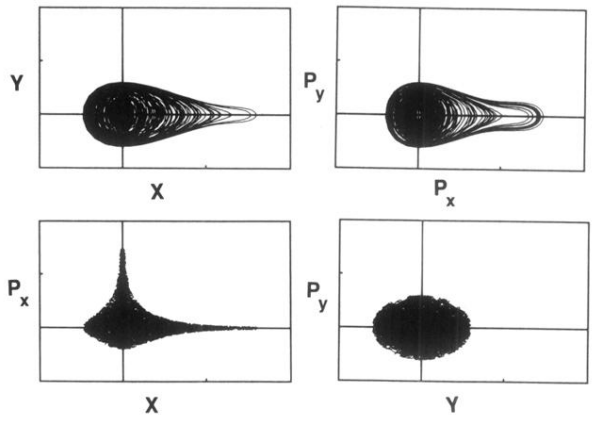

FIG. 3. Trajectory no. 1 along various cross sections of the phase space.

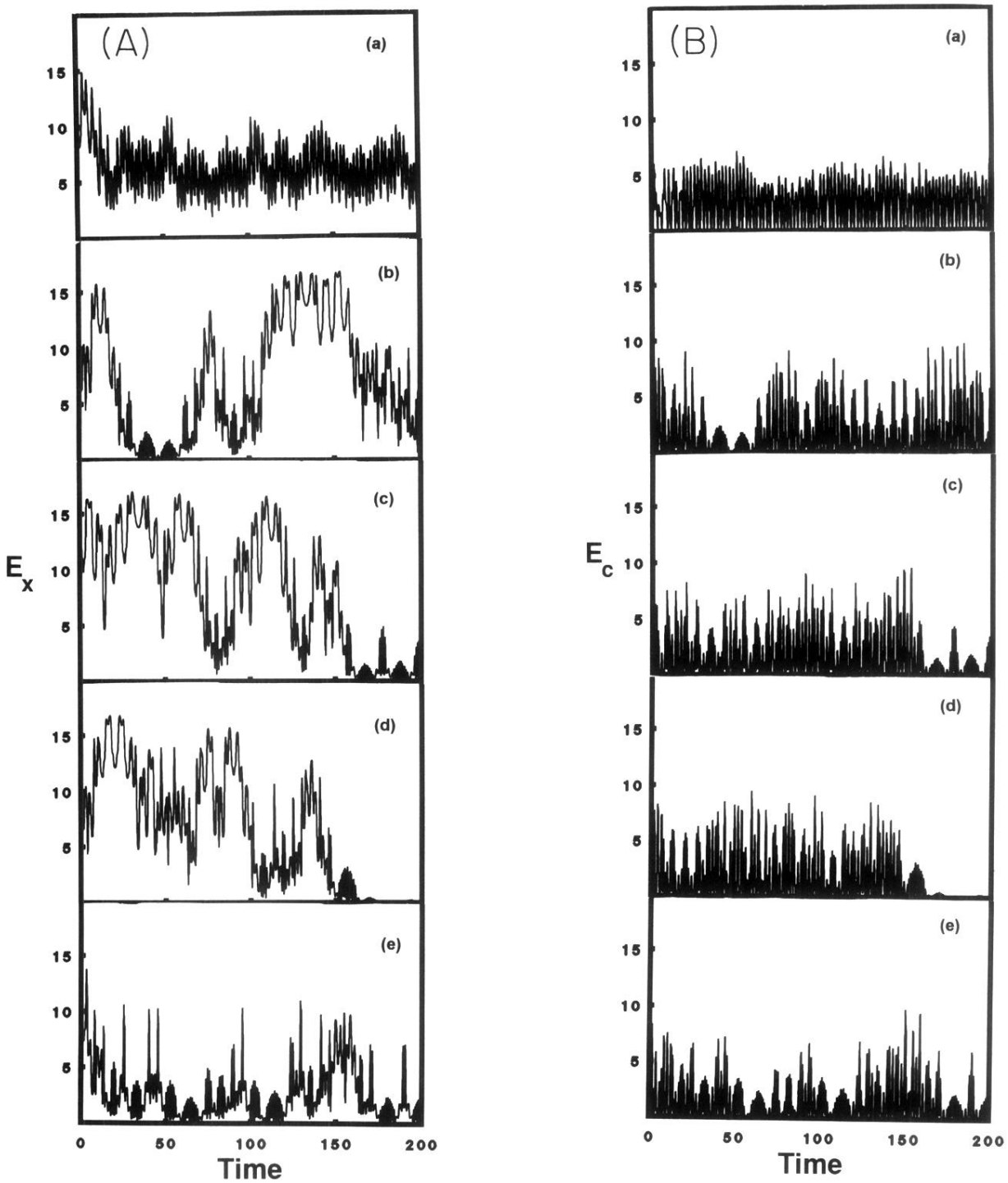

FIG. 4. (A) E_x for FC and MM trajectories. (a) Mixed mode, (b) trajectory no. 1, (c) trajectory no. 2, (d) trajectory no. 3, (e) trajectory no. 4. (B) E_c for FC and MM trajectories. (a) Mixed mode, (b) trajectory no. 1, (c) trajectory no. 2, (d) trajectory no. 3, (e) trajectory no. 4.

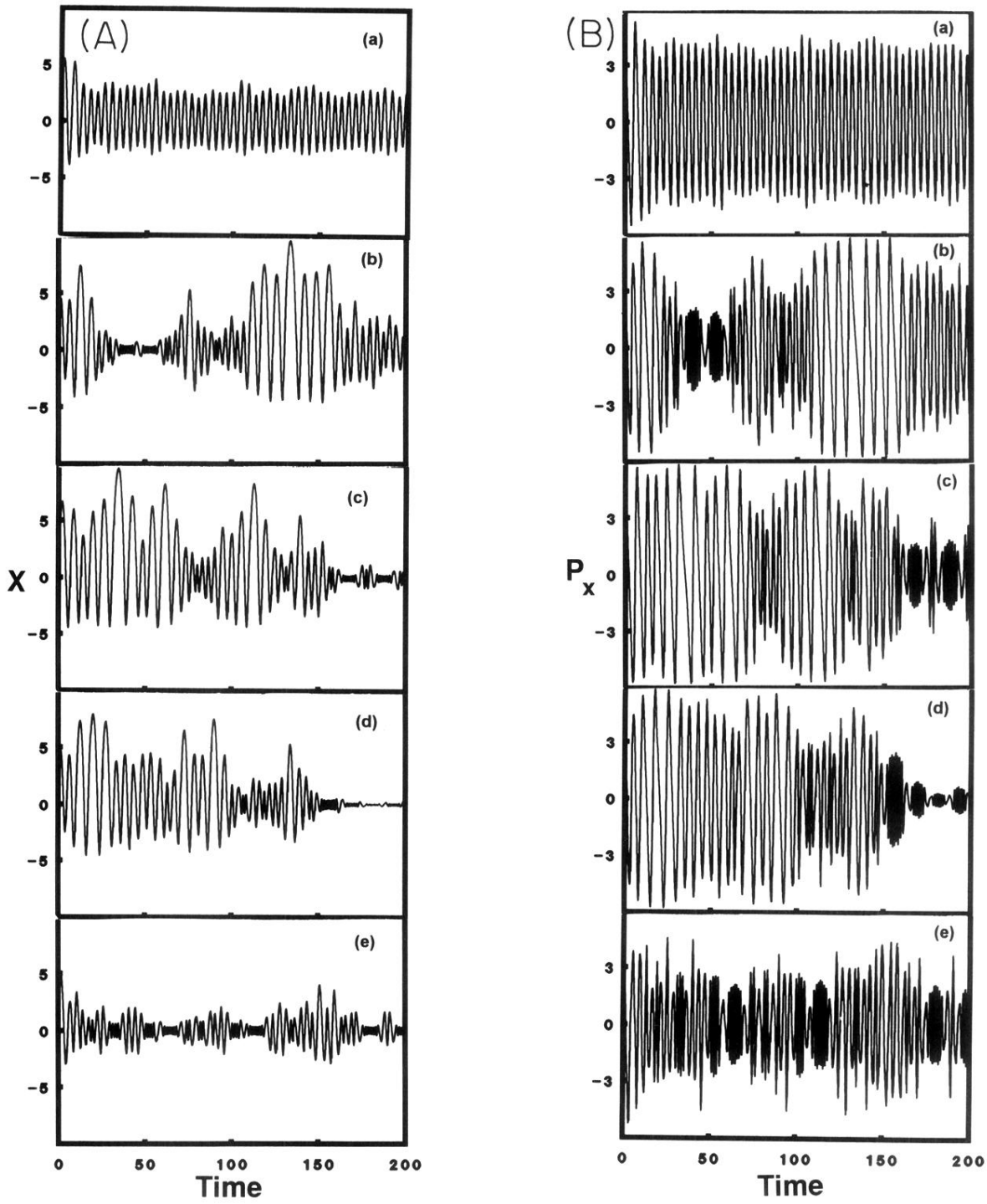

FIG. 5. (A) x for FC and MM trajectories. (a) Mixed mode, (b) trajectory no. 1, (c) trajectory no. 2, (d) trajectory no. 3, (e) trajectory no. 4. (B) p_x for FC and MM trajectories. (a) Mixed mode, (b) trajectory no. 1, (c) trajectory no. 2, (d) trajectory no. 3, (e) trajectory no. 4.

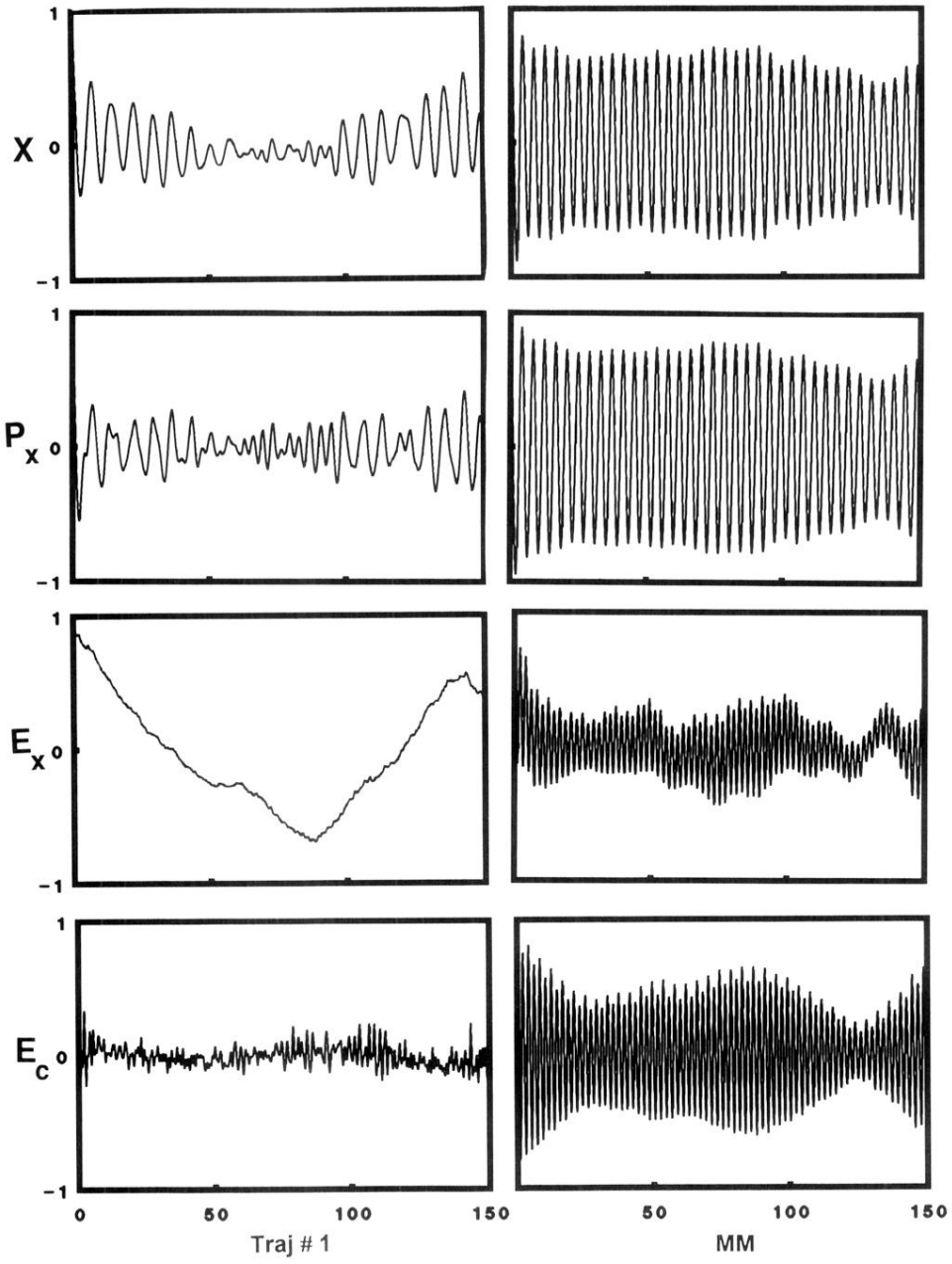

FIG. 6. Autocorrelation functions of x, P_x, E_x, and E_c for the classical trajectory no. 1 and MM.